AIP | Applied Physics Letters

A miniaturized piezoelectric turbine with self-regulation for increased air speed range

Hailing Fu and Eric M. Yeatman

Citation: Applied Physics Letters **107**, 243905 (2015); doi: 10.1063/1.4938000
View online: http://dx.doi.org/10.1063/1.4938000
View Table of Contents: http://scitation.aip.org/content/aip/journal/apl/107/24?ver=pdfcov
Published by the AIP Publishing

A miniaturized piezoelectric turbine with self-regulation for increased air speed range

Hailing Fu[a] and Eric M. Yeatman
Department of Electrical and Electronic Engineering, Imperial College London, London SW7 2AZ, United Kingdom

(Received 21 October 2015; accepted 1 December 2015; published online 14 December 2015)

This paper presents the design and demonstration of a piezoelectric turbine with self-regulation for increased air speed range. The turbine's transduction is achieved by magnetic "plucking" of a piezoelectric beam by the passing rotor. The increased speed range is achieved by the self-regulating mechanism which can dynamically adjust the magnetic coupling between the magnets on the turbine rotor and the piezoelectric beam using a micro-spring. The spring is controlled passively by the centrifugal force of the magnet on the rotor. This mechanism automatically changes the relative position of the magnets at different rotational speeds, making the coupling weak at low airflow speeds and strong at high speeds. Hence, the device can start up with a low airflow speed, and the output power can be ensured when the airflow speed is high. A theoretical model was established to analyse the turbine's performance, advantages, and to optimize its design parameters. A prototype was fabricated and tested in a wind tunnel. The start-up airflow speed was 2.34 m/s, showing a 30% improvement against a harvester without the mechanism. [http://dx.doi.org/10.1063/1.4938000]

Due to the decreasing power consumption of microelectronics, the concept of autonomous sensing devices is realizable by harnessing the wasted ambient energy for power supply. Airflow is a widespread energy source in many domestic and industrial situations, including ventilation systems, mining tunnels, and moving vehicles, where wireless sensor nodes are often installed.[1–3] Hence, airflow energy harvesters are potential alternatives to conventional batteries for wireless sensing devices.

Airflow energy harvesting using miniaturized turbines has drawn significant interest for the past years.[4,5] Holmes *et al*. demonstrated a millimeter-scale turbine using microfabrication.[6] Priya *et al*. developed a piezoelectric energy harvester using a windmill structure.[7] Fu and Yeatman adapted the magnetic plucking method into a piezoelectric turbine to achieve the non-contact plucking of piezoelectric beams.[8] However, the start-up airflow speed is still a main barrier for these harvesters to extract airflow energy at low speeds. Howey *et al*. employed high-quality jewel bearings to minimize the friction,[9] but the main resistance in these devices is still given by the magnetic coupling force. Kishore *et al*. adopted large-size blades to generate a higher driving torque at low speeds,[10] which is undesirable for small-scale devices.

A feasible way to decrease the start-up speed and to maintain the output power at high speeds is to alter the magnetic coupling automatically along with the airflow speed. Self-regulating mechanisms, as a potential solution, have been used in many energy harvesting devices.[11–15] Lallart *et al*. developed a broadband vibration energy harvester using additional sensing and actuating components to adjust the resonant frequency of the beam along with the excitation frequency.[11] The bandwidth of the structure improved significantly, but the generated power was partially consumed by these components. Miller *et al*. built a self-tuning vibration energy harvester by mounting a sliding proof mass on a clamped-clamped beam.[13] The position of the mass adjusts automatically with respect to vibration frequency, extending the bandwidth of the device. Gu and Livermore designed a rotational self-regulating energy harvester by adjusting the beam's tensile stress generated by the centrifugal force.[15] The stress adjusted the stiffness and the resonant frequency of the beam, enabling the resonant frequency to be identical to the excitation frequency in a wide operating range. By adopting a suitable self-regulating method, a piezoelectric turbine with a low start-up airflow speed was designed and is presented in this paper.

The schematic of the turbine is illustrated in Fig. 1. The self-regulating mechanism is achieved by changing the magnetic coupling in respond to the airflow speed using a spring-centrifugal governor system, enabling the device to start up at low airflow speed and to enhance the output power at high speeds.

The magnetic coupling is realized by two magnets in the harvester: one on the beam's free end and the other on the rotor's rear plate. The centrifugal governor is the sliding magnet supported by two sliders on rails. The magnet is

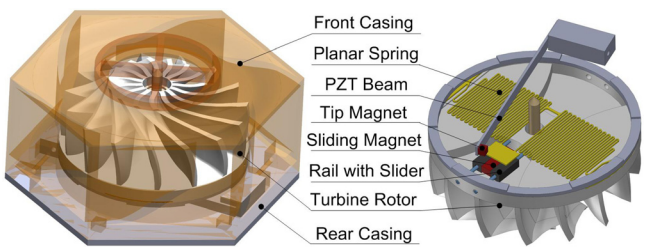

FIG. 1. Design of the micro piezoelectric turbine, showing the implementation of the self-regulating mechanism.

[a]Electronic mail: h.fu14@imperial.ac.uk

rigidly connected with a spring which is designed to control the radial position of the magnet.

The schematic of the self-regulating system is shown in Fig. 2(a). In a windless condition, the device is stationary with the spring unstretched. The gap between the magnets is correspondingly large, ensuring that the coupling is weak enough for the turbine to start up at a low airflow speed. When the airflow speed is increased and the rotational speed of the rotor rises, the centrifugal force generated by the rotating magnet increases. As the spring is stretched, the gap decreases, intensifying the magnetic coupling and improving the output power.

If we assume that the turbine is activated by airflow and operates at a rotational frequency of ω_{tr}, then the gaps between magnets in 3 axes are

$$d_x = r_{m0} + d_{x0} - r_m \cos(\omega_{tr} t - \alpha_{m0}), \tag{1a}$$

$$d_y = r_m \sin(\omega_{tr} t - \alpha_{m0}) - \omega(L,t), \tag{1b}$$

$$d_z = d_{z0}, \tag{1c}$$

where d_{x0} and d_{z0} are the initial gaps along the x-axis and z-axis when the rotor is static, with the sliding magnet's angular position $\alpha_{m0} = 0$, $\omega(L,t)$ is the tip displacement of the piezoelectric beam in the y direction, and r_m is the rotational radius of the sliding magnet, which is given by

$$r_m = \frac{k_s r_{m0}}{k_s - m_{sm}\omega_{tr}^2}, \tag{2}$$

where k_s is the spring constant, r_{m0} is the initial radius of the sliding magnet, and m_{sm} is the mass of the sliding magnet.

The magnetic coupling force, F^y_{mag}, in the beam vibration direction can be calculated numerically using the theory given by Akoun and Yonnet.[16] The configuration of the magnet coupling is illustrated in Fig. 2(b). The magnetic force between two cuboidal magnets in the beam vibration direction can be calculated using

$$F^y_{mag} = \frac{J \cdot J'}{4\pi\mu_0} \sum_{i=0}^{1}\sum_{j=0}^{1}\sum_{k=0}^{1}\sum_{l=0}^{1}\sum_{p=0}^{1}\sum_{q=0}^{1} (-1)^{i+j+k+l+p+q} \cdot \phi_y, \tag{3}$$

where J and J' are the magnetization of magnets, μ_0 is the magnetic constant, and ϕ_y is a function of the magnet dimensions and their gaps in 3 axes. The function is given by

$$\phi_y = \frac{1}{2}\left(U_{ij}^2 - W_{pq}^2\right)\ln(r - V_{kl}) + U_{ij}Vkl\ln(r - U_{ij}) + U_{ij}W_{pq}\tan^{-1}\left(\frac{U_{ij}V_{kl}}{rW_{pq}}\right) + \frac{1}{2}rV_{kl}, \tag{4}$$

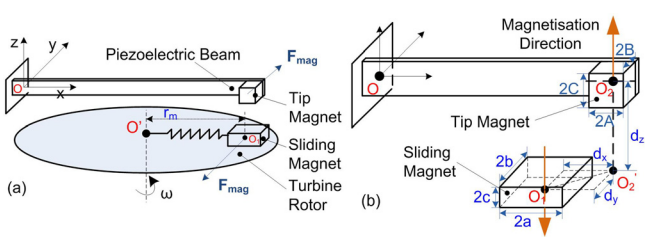

FIG. 2. (a) Schematic of the self-regulating turbine and (b) magnetic coupling configuration.

where

$$U_{ij} = d_x + (-1)^j A - (-1)^i a, \tag{5a}$$

$$V_{kl} = d_y + (-1)^l B - (-1)^k b, \tag{5b}$$

$$W_{pq} = d_z + (-1)^q C - (-1)^p c, \tag{5c}$$

$$r = \sqrt{U_{ij}^2 + V_{kl}^2 + W_{pq}^2}. \tag{5d}$$

These lengths, U_{ij}, V_{kl}, and W_{pq}, correspond to the distance between the cube corners and their projections on the axes. The parameters i, j, k, l, p, and q, are equal to 0 or 1 according to the specific corner.

The magnetic force on the tip magnet excites the piezoelectric beam once per cycle. Erturk and Inman established a comprehensive theoretical model for the beam operating with base excitation.[17] By adapting this theory to tip force excitation, the coupling equations describing the motion of the beam are given as follows:

$$YI\frac{\partial^4\omega(x,t)}{\partial x^4} + c_s I\frac{\partial^5\omega(x,t)}{\partial^4 x\partial t} + c_d\frac{\partial\omega(x,t)}{\partial t} + m\frac{\partial^2\omega(x,t)}{\partial t^2} - \vartheta v(t)\left[\frac{d\delta(x)}{dx} - \frac{d\delta(x-L)}{dx}\right] = F^y_{mag}(t), \tag{6}$$

and

$$\frac{C_p}{2}\frac{dv(t)}{dt} + \frac{v(t)}{R_l} + \bar{e}_{31}\frac{h_p + h_s}{2}b\int_0^L \frac{\partial^3\omega(x,t)}{\partial x^2\partial t} = 0, \tag{7}$$

where YI is the bending stiffness, $\omega(x,t)$ is the transverse deformation of the beam, $c_s I$ is the internal damping, c_d is the viscous deformation damping, m is the mass per unit length of the beam, δ_x is the Dirac delta function, ϑ is the piezoelectric coupling term in physical coordinates, $v(t)$ is the voltage across a resistive load R_l, C_p is the inherent capacitance of the piezoelectric beam, $\bar{e}_{31}$ is the piezoelectric constant, h_p and h_s are the height of the piezoelectric layer and the substrate layer, respectively, b is the width of the beam, and L is the length of the beam.

The performance of the piezoelectric turbine was analysed theoretically using the above analysis. A device was designed with the parameters listed in Table I. Fig. 3 illustrates the regulating behaviour and the operating principle of the harvester based on the above equations and parameters. The system has a weak magnetic coupling at low frequencies

TABLE I. Design parameters of the piezoelectric turbine.

Symbol	Description	Value
$L \times b$	Beam size	26.5 mm × 1.5 mm
h_p	Thickness of piezo layer	0.1 mm
h_s	Thickness of substrate	0.1 mm
r_t	Radius of turbine rotor	27 mm
$a \times b \times c$	Sliding magnet size	$2.5 \times 0.75 \times 0.5\ \text{mm}^3$
$A \times B \times C$	Tip magnet size	$0.5 \times 0.5 \times 0.5\ \text{mm}^3$
d_{z0}	Initial gap in z-axis	3.2 mm
J	Magnetization of magnets	1.17 T
ρ_m	Density of magnets	$7400\ \text{kg/m}^3$
$\bar{e}_{31}$	Piezoelectric constant	−22.2 V × m/N
r_{m0}	Spring free length	8 mm

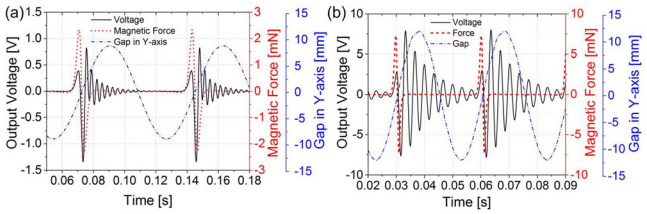

FIG. 3. Simulated results: Gap between the magnets, magnetic force, and output voltage of the piezoelectric turbine. (a) Operating at 13.8 Hz and (b) operating at 33 Hz ($k_s = 8.5$ N/m).

(13.8 Hz in Fig. 3(a)), which enables the system to start up at low airflow speeds. The coupling is enhanced at high frequencies (33 Hz) by the centrifugal force of the sliding magnet, allowing the output power to be improved.

The spring constant is a critical parameter determining the self-regulating behaviour. In order to decrease the start-up airflow speed and to intensify the magnetic coupling quickly after start-up, the behaviour was investigated with different spring constants k_s. The initial length, r_{m0}, of the spring is 8.2 mm and the initial gap, d_{x0}, of the magnet in the x direction is 3.8 mm. The regulating behaviour initiates when the turbine starts operating and terminates at the maximum magnetic coupling ($r_m = r_{m0} + d_{x0}$) by a mechanical stopper on the spring.

As illustrated in Fig. 4, the magnetic coupling after the regulating stage is 6 times higher than that in the initial stage, which indicates the effect of the regulating mechanism. The range of the self-regulating behaviour depends on the spring constant, extending with increasing spring constant. In this mechanism, the regulating range should be as narrow as possible in order to enhance the output power after start-up. The spring constant, therefore, should be low enough to fulfil the requirement.

In order to achieve a low spring constant, a micro planar tensile spring was fabricated from titanium foil by laser machining. The width and thickness of the spring beam are 110 μm and 200 μm, respectively. The spring constant was measured as 2.28 N/m. The self-regulating mechanism is implemented by the partial assembly in Fig. 5(a). The turbine rotor and casing were built from Verowhite Plus material using the 3D printer Stratasys Objet 500 Connex 3. The assembled prototype is presented in Fig. 5(b). The turbine has six inlets arranged on the lateral sides of the hexagonal

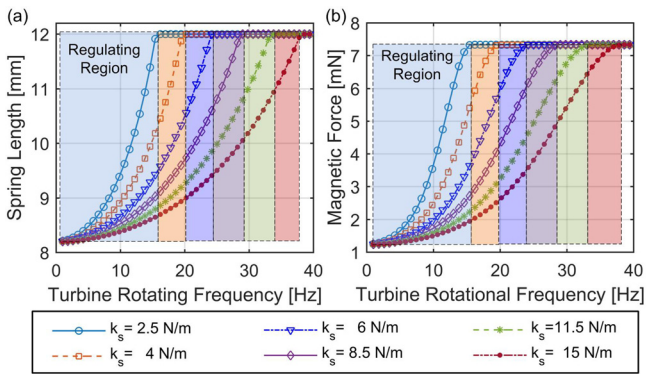

FIG. 4. Simulated self-regulating behaviour with different spring constants. (a) Spring length versus turbine rotational frequency and (b) peak magnetic force in the y direction versus rotational frequency.

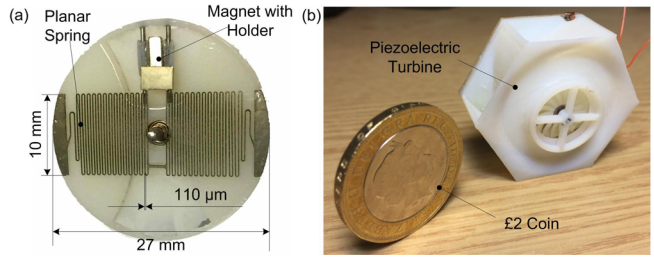

FIG. 5. Prototype. (a) Implementation of the self-regulating mechanism and (b) piezoelectric turbine (ø37 mm × 18 mm).

prism casing, allowing the device to operate with airflow from any direction. The inlets work as concentrators with the cross-sectional area narrowed down as the airflow gets into the turbine.

The prototype was tested in a miniature wind tunnel. Its schematic is shown in Fig. 6; it is an open loop wind tunnel with continuously variable airspeed control. It comprises four major components: contraction, test section, diffuser, and fan. Airflow enters the tunnel from the contraction section and exits from the diffuser. The performance of the harvester was measured in the test section, whose dimension is 100 mm × 85 mm × 85 mm. A pitot tube used to measure the airflow speed was installed in parallel with the harvester in the test section.

The turbine was tested against load resistance and airflow speed. The optimal load resistance of the device is 100 kΩ, as shown in Fig. 7. The maximum peak power output at 3.94 m/s airflow speed is 705 μW.

In order to validate the self-regulating mechanism, the device was tested at varied airflow speeds. Fig. 8 depicts the peak output power and the rotational frequency of the turbine rotor against airflow speed. The start-up airflow speed of the device is 2.34 m/s and the regulating behaviour terminates at 4.21 m/s, where a 742 μW peak output power was measured

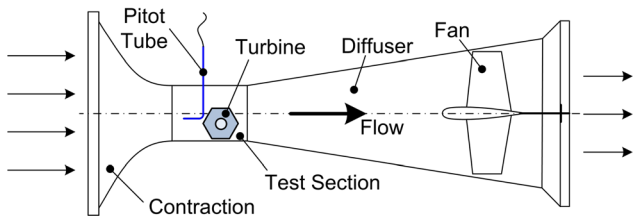

FIG. 6. Schematic of the experimental set-up.

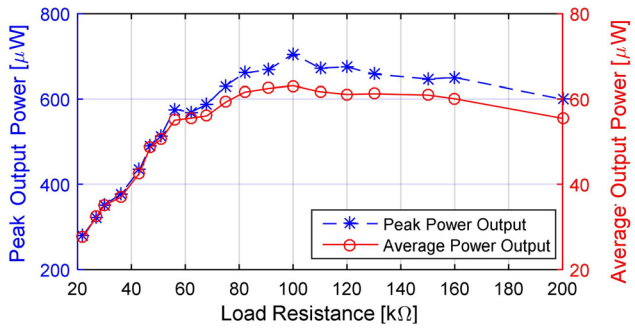

FIG. 7. Peak and average output power of the harvester versus load resistance at 3.94 m/s airflow speed.

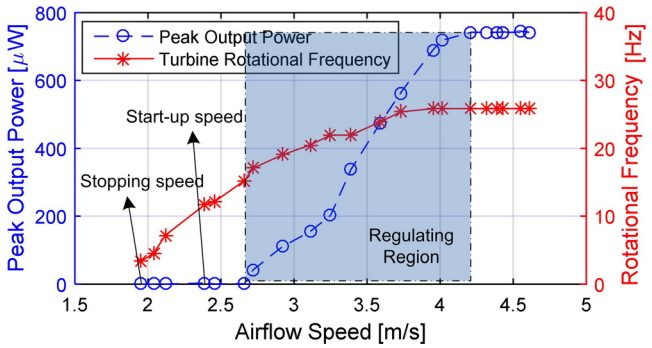

FIG. 8. Peak average output power and rotational frequency of the harvester with a 100 kΩ load versus airflow speed.

TABLE II. Power density and start-up speed of airflow energy harvesters.

Device	Transduction[a]	Dimension (mm)	Power density[b]	Start-up speed
Ref. 5	T and PE	96 × 254 × 127	1.615	2.41 m/s
Ref. 8	T and PE	47 × 42 × 25	2.533	3.5m/*s*
Ref. 9	T and EM	ø32 × 50	7.460	3 m/s
Ref. 10	T and PE	100 × 80 × 65	0.865[c]	1.1 m/s
Ref. 19	T and PE	80 × 80 × 175	0.446	2.0 m/s
Ref. 20	PE	100 × 60 × 30	1.389	3.6 m/s
Ref. 21	PE	141 × 100 × 55	1.676	2.5 m/s
Ours	T and PE	ø37 × 18	4.480[d]	2.34 m/s

[a]T—Turbine, PE—Piezoelectric, and EM—Electromagnetic.
[b]The air speed is 4 m/s, and the unit is μW/cm^3.
[c]The air speed is 1.9 m/s. The power density is lower at 4 m/s.
[d]The average output power of 71.7 μW was obtained at 4 m/s airflow speed with a 100 kΩ resistor.

with a 100 kΩ load. The frequency up-conversion mechanism[8,18] employed in this device addresses the falling-off of output power caused by frequency mismatching at high airflow speeds observed by Karami *et al.*[19]

The device without the self-regulating mechanism was also tested. The start-up airflow speed was 3.35 m/s. It indicates that the self-regulating mechanism has reduced the requirement of the start-up airflow speed to 30%. Compared to other airflow energy harvesters, this piezoelectric turbine also shows improved performance in power density and start-up airflow speed (Table II). The design from Howey *et al.*[9] has the highest power density; however, the structure is complex and the cost for fabrication is likely to be much higher. In addition, the power density using electromagnetic conversion is in the same order as the density using piezoelectric conversion in this paper. The power density in this paper is 4.48 μW/cm^3, which can be further improved by integrating multiple piezoelectric beams and optimizing the structure of the device. The design from Kishore *et al.*[10] has the lowest start-up speed, but the size is higher and the power density is the lowest. The start-up speed of the device in this paper can be decreased by minimizing the frictions.

In conclusion, a piezoelectric turbine aiming at extracting airflow energy at low speeds is presented in this paper. A passive self-regulating mechanism is implemented by dynamically adjusting the magnetic coupling between the two magnets on the turbine rotor and the piezoelectric beam using a micro spring. The device, therefore, can start up with a low airflow speed and the output power can be ensured when the airflow speed is high. A theoretical model was established to analyse the turbine's performance, advantages, and to optimize its design parameters. A prototype was fabricated and tested in a wind tunnel. The start-up airflow speed was 2.34 m/s, showing a 30% improvement against the untuned harvester. The piezoelectric turbine has an improved performance against other harvesters in terms of power density and start-up airflow speed.

The work was supported by the Department of Electrical and Electronic Engineering, Imperial College and the China Scholarship Council. We would also like to thank Professor Andrew Holmes for use of apparatus.

[1]J. W. Matiko, N. J. Grabham, S. P. Beeby, and M. J. Tudor, Meas. Sci. Technol. **25**, 012002 (2014).
[2]P. H. Mellor, S. G. Burrow, T. Sawata, and M. Holme, IEEE Trans. Ind. Appl. **41**, 551 (2005).
[3]P. D. Mitcheson, E. M. Yeatman, G. K. Rao, A. S. Holmes, and T. C. Green, Proc. IEEE **96**, 1457 (2008).
[4]A. S. Holmes, "Energy harvesting from fluid flows," in *Micro Energy Harvesting* (Wiley, 2015), pp. 297–319.
[5]R. Myers, M. Vickers, H. Kim, and S. Priya, Appl. Phys. Lett. **90**, 054106 (2007).
[6]A. Holmes, G. Hong, and K. Pullen, J. Microelectromech. Syst. **14**, 54 (2005).
[7]S. Priya, C.-T. Chen, D. Fye, and J. Zahnd, Jpn. J. Appl. Phys., Part 2 **44**, L104 (2005).
[8]H. Fu and E. M. Yeatman, "A miniature radial-flow wind turbine using piezoelectric transducers and magnetic excitation," J. Phys.: Conf. Ser. (to be published).
[9]D. A. Howey, A. Bansal, and A. S. Holmes, Smart Mater. Struct. **20**(8), 085021 (2011).
[10]R. A. Kishore, D. Vukovi, and S. Priya, Ferroelectrics **460**, 98 (2014).
[11]M. Lallart, S. R. Anton, and D. J. Inman, J. Intell. Mater. Syst. Struct. **21**, 897 (2010).
[12]S. Roundy and Y. Zhang, Proc. SPIE **5649**, 373 (2005).
[13]L. M. Miller, P. Pillatsch, E. Halvorsen, P. K. Wright, E. M. Yeatman, and A. S. Holmes, J. Sound Vib. **332**, 7142 (2013).
[14]V. R. Challa, M. G. Prasad, and F. T. Fisher, Smart Mater. Struct. **20**, 025004 (2011).
[15]L. Gu and C. Livermore, Appl. Phys. Lett. **97**, 081904 (2010).
[16]G. Akoun and J.-P. Yonnet, IEEE Trans. Magn. **20**, 1962 (1984).
[17]A. Erturk and D. J. Inman, Smart Mater. Struct. **18**, 025009 (2009).
[18]P. Pillatsch, E. M. Yeatman, and A. S. Holmes, Sens. Actuators A: Phys. **206**, 178 (2014).
[19]M. A. Karami, J. R. Farmer, and D. J. Inman, Renewable Energy **50**, 977 (2013).
[20]S.-D. Kwon, Appl. Phys. Lett. **97**, 164102 (2010).
[21]D. Zhu, S. Beeby, M. Tudor, N. White, and N. Harris, IEEE Sens. J. **13**, 691 (2013).